HGT

Lentiviral Gene Therapy for Familial Hemophagocytic Lymphohistiocytosis Type 3, Caused by *UNC13D* Genetic Defects

Sarah E. Takushi,[1–3] Na Yoon Paik,[2,3] Andrew Fedanov,[2,3] Chengyu Prince,[2,3] Christopher B. Doering,[2–4] H. Trent Spencer,[2–4] and Shanmuganathan Chandrakasan[2,3,5,*]

[1]*Department of Immunology and Molecular Pathogenesis, Graduate Division of Biological and Biomedical Sciences, Laney Graduate School, Emory University, Atlanta, Georgia, USA.*
[2]*Cell and Gene Therapy Program, Aflac Cancer and Blood Disorders Center, Children's Healthcare of Atlanta, Atlanta, Georgia, USA.*
[3]*Department of Pediatrics, Emory University, Atlanta, Georgia, USA.*
[4]*Department of Molecular and Systems Pharmacology, Graduate Division of Biological and Biomedical Sciences, Emory University School of Medicine, Atlanta, Georgia, USA.*
[5]*Bone Marrow Transplant Program, Aflac Cancer and Blood Disorders Center, Children's Healthcare of Atlanta, Atlanta, Georgia, USA.*

Familial hemophagocytic lymphohistiocytosis type 3 (FHL3) is a rare disease caused by mutations to the *UNC13D* gene and the subsequent absence or decreased activity of the Munc13-4 protein. Munc13-4 is essential for the exocytosis of perforin and granzyme containing granules from cytotoxic cells. Without it, these cells are able to recognize an immunological insult but are unable to execute their cytotoxic functions. The result is a hyperinflammatory state that, if left untreated, is fatal. At present, the only curative treatment is hematopoietic stem cell transplantation (HSCT), but eligibility and response to this treatment are largely dependent on the ability to control inflammation before HSCT. In this study, we describe an optimized lentiviral vector that can restore Munc13-4 expression and degranulation capacity in both transduced FHL3 patient T cells and transduced hematopoietic stem cells from the FHL3 (*Jinx*) disease model.

Keywords: FHL3, HLH, *UNC13D*, Munc13-4, lentiviral vector

INTRODUCTION

Hemophagocytic lymphohistiocytosis (HLH) is typified by high fever, splenomegaly, cytopenias, hypertriglyceridemia and/or hypofibrinogenemia, hemophagocytosis, reduced NK cell activity, high ferritin levels, elevated levels of sIL2R,[1,2] and often hyponatremia.[3,4] In its inherited form, HLH is caused by mutations to the *PRF1*, *UNC13D*, *STX11*, *STXBP2*, and other genes that are associated with the exocytosis of lytic granules from cytotoxic cells. Consequently, infants with HLH are born seemingly healthy, but upon encountering an immunological insult such as a viral infection (*e.g.*, Epstein-Barr virus [EBV]), their lymphocytes cannot execute cytotoxic degranulation, leading to a positive feedback loop of massive inflammation without clearing the infectious trigger.[5–7] Left untreated, the disease is fatal.[8,9] To date, the only curative treatment available is an allogenic hematopoietic stem cell transplantation (HSCT). However, inflammation must be adequately controlled before HSCT, and despite recommendations for intensification of therapy in the HLH-2004 international treatment study, the reported pre-HSCT mortality was still high at 19%.[9] Survival rates vary depending on the conditioning protocol.[10–19] Thus far, results from clinical trial NCT01998633 suggest that reduced intensity conditioning can improve overall 1-year survival of HLH patients to 82.4%, although larger and longer term studies will be needed to follow-up on these results.[20] For patients who do receive HSCT, the 5-year survival rate has improved from 54% to 61%.[16–18,21] Thus, despite several advances made in the field of HLH disease treatment, the outcome is suboptimal and there is still substantial room for improvement.

HLH has been proposed as an excellent candidate for hematopoietic stem and progenitor cell (HSPC)-based gene therapy intervention for several reasons. First, modification of a patient's own HSPC would reconstitute immune system with functional cytotoxic cells, theoretically correcting the HLH phenotype for life. Second, this autologous HSPC-based gene therapy could eliminate the risk of graft versus host disease compared with an allo-

*Correspondence: Dr. Shanmuganathan Chandrakasan, Bone Marrow Transplant Program, Aflac Cancer and Blood Disorders Center, Children's Healthcare of Atlanta, 2015 Uppergate Drive, Atlanta, GA 30322, USA. E-mail: shanmuganathan.chandrakasan@emory.edu

DOI: 10.1089/hum.2019.329

genic HSCT. Third, patients who receive an HLH diagnosis would not have to wait to find a matching HSCT donor. Finally, modification of a patient's own T cells could be used in autologous adoptive transfer to control infection and inflammation before HSCT.[22–24]

In this study, we focused exclusively on lentiviral (LV) gene therapy for familial HLH type 3 (FHL3), which is caused by mutations to the *UNC13D* gene and a subsequent absence or loss of function in the Munc13-4 protein. Studies conducted in Germany and North America found that FHL3 accounts for ~25–30% of inherited HLH cases.[25,26] FHL3 is the most common form of FHL documented in white patients,[26] although multiple independent founder mutations leading to FHL3 have been described in populations from around the world.[26–30] Missense and nonsense mutations, deletions, splicing error variants, and inversions have all been described in FHL3 patients, and no single exon of the 32 spliced exons seems to be favored as a site for mutation.[31,32]

Munc13-4 is part of the UNC13 family of proteins, all of which are involved in processes relating to vesicle exocytosis. Munc13-4 has been implicated in the exocytosis of lytic granules from cytotoxic cells,[8,33] tertiary, and mucin-containing granules from neutrophils,[34,35] dense granules from platelets,[36] and secretory granules from mast cells during regulated exocytosis.[37] Although much of HLH research has focused on pathology arising from impairment of CD8 T cell and natural killer cell cytotoxic function,[8] it is worth noting that FHL3 patients also suffer from susceptibility to fungal infection,[38] neurological symptoms,[39] exacerbated response to lung infection,[26,39] and macrophage activation syndrome,[26] which could be related to impaired degranulation from other cell types. Although Munc13-4 is expressed in other tissues,[40–42] the fact that HSCT results in cure suggests that its most critical role is in cells derived from the hematopoietic lineage, and therefore its role in nonhematopoietic tissues might be limited or complemented by other proteins in degranulation pathways.

The first gene therapy study for FHL3 was recently published and described by transducing activated peripheral blood mononuclear cells (PBMCs) from three FHL3 patients using either a vesicular stomatitis virus G protein (VSV-G) or a measles H/F pseudotyped LV vector that encoded for the complementary DNA (cDNA) product from the human *UNC13D* gene. When NSG mice were transplanted with EBV-induced tumors and then infused with transduced FHL3 patient T cells, reduction in tumor size was observed.[24] The same group then showed transduction of hematopoietic stem cells from Munc13-4 null (*Jinx*) mice—the mouse model for FHL3—showed improvements to *in vitro* metrics and viral clearance as a result of gene therapy.[23] Finally, a second group transduced FHL3 patient cells with a gamma retrovirus-based gene therapy construct demonstrated that transduced cells had improved degranulation capacity and cytotoxic abilities.[22] Both groups used an Ef1α promoter and codon-optimized transgene.[22,23] Here, we describe several new LV vectors, establish the minimum chimeric threshold needed for restoring adequate degranulation, and demonstrate that our described vector can be used to transduce both patients T cells and HSPC from the FHL3 mouse model.

MATERIALS AND METHODS

Cloning

All cloning was carried out into the LTG 1337 backbone, supplied by Expression Therapeutics. In humans, *UNC13D* comprises 32 exons,[8] therefore in constructing our *UNC13D* LV vector, we used the sequence from the *Homo sapiens* unc-13 homolog D (*UNC13D*) messenger RNA (mRNA; NCBI reference Sequence: NM_199242.2). When translated, this nucleotide sequence yields isoform 1 of the Munc13-4 protein (protein Sequence NP_954712.1, UniProt identifier Q70J99-1). Codon optimization was performed by GenScript according to the algorithm previously described in our laboratory.[43] All clones were screened using restriction digest and sequenced by Genewiz.

LV vector packaging and titering

The third generation, self-inactivating, VSV-G pseudotyped LV vectors were constructed using a standard HEK 293T transfection protocol.[44] Specifically, HEK 293 T/17 cells were transfected with a four-plasmid system. After transfection, the following day the media was replaced with Dulbecco's modified Eagle's medium (DMEM), 1× with 4.5 g/L glucose, L-glutamine and sodium pyruvate, supplemented with 10% fetal bovine serum (FBS). Supernatant from these transfected cells was collected on day 2 and 3 post-transfection. Viral vector was pelleted by overnight ultracentrifugation at 10,000 *g*, 4°C. Pelleted viral vector was subsequently filtered through a 0.22 μm filter and resuspended in StemPro media. All LV vector preparations were titered by applying polybrene (aka ''hexadimethrene bromide,'' 8 μg/mL; Sigma) and 3, 9, or 27 μL of the LV vector onto HEK 293T/17 cells, incubating overnight, and then culturing in fresh media for 5 days. DNA was subsequently isolated from these cells using a Qiagen DNA Micro kit (56304; Qiagen). Quantitative polymerase chain reaction (qPCR) was performed using Power SYBR Green Master Mix (4367659; ThermoFisher) with RRE primers (forward primer: TGG AGT GGG ACA GAG AAA TTA ACA, reverse primer: GCT GGT TTT GCG ATT CTT CAA) to determine the average number of copies of viral vector DNA that were integrated per cell.

Transduction

All transductions were carried out in the presence of polybrene-supplemented media (8 μg/mL; Sigma). Cell lines used in *in vitro* experiments were transduced once with a single overnight application of LV vector using the

specified multiplicity of infections (MOIs). HSCs that were used for transplant studies were transduced twice in 50% viral media (mean MOI of 42), with the first hit of the virus being incubated on the cells overnight and the second hit of virus lasting for 6 h.

Transplants

Whole bone marrow was flushed from the tibias and femurs of donor *Jinx* (Unc13d^{Jinx}, *UNC13D*; Jackson Laboratories) or CD45.1^{+} mice. Sca-1^{+} cells were isolated according to manufacturer protocols using Sca-1 antibody (553334; BD Biosciences), biotin-labeled magnetic beads (130-090-485; MACS; Miltenyi Biotec), and MACS magnetic separation unit (Miltenyi Biotec magnet and stand; 130-042-303 and 130-042-109, respectively). These isolated Sca-1 cells were then cultured in stimulation media consisting of StemPro nutrient-supplemented media (10640-019; Gibco), recombinant mouse interleukin 3 (IL-3) (20 ng/mL; 403-ML; R&D), recombinant human IL-11 (100 ng/mL; 218-IL; R&D), recombinant human Flt3/Fc (100 ng/mL; 368-ST; R&D), mouse mSCF (100 ng/mL; 455 MC; R&D), L-glutamine (SH30034.01; HyClone), and penicillin and streptomycin (09-757F; Lonza). These cells were subsequently transduced with the specified LV gene therapy vector. Before transplantation, recipient mice were kept on antibiotic water for 1 week and were lethally irradiated using two 550 rad doses of gamma radiation. For the transplantation, recipient mice received 1 million transduced Sca-1 cells through retro-orbital injection and kept on antibiotic water for 2 weeks post-transplantation.

VCN analysis

The same RRE primers, SYBR Green Power PCR Master Mix, and PCR protocol that were used for the titering of new LV vectors were also used in the qPCR-based copy number analysis of transduced cells.

Infection

Jinx mice were infected by intraperitoneal injection with 2×10^5 plaque-forming units (PFU) of lymphocytic choriomeningitis virus (LCMV) Armstrong (generously provided by the Ahmed Lab).

Colony-forming unit assays

One thousand cells per milliliter of Methocult Culture media (03434; StemCell Technologies) were plated and incubated for 7–10 days. Colonies were subsequently counted, assessed using a viability stain, and the number of successfully transduced colony-forming units was determined either by copy number assay or flow cytometry on the pooled cells.

Western blot

A standard Western blot protocol[45] was performed by blotting onto a PVDF membrane (162-0261; BioRad) and staining for Munc13-4 (Clone ERP4914, ab109113; Abcam) and beta-actin (Clone 2D1D10, A00702; GenScript). Secondary antibodies (IRDye 800 CW and IRDye 680; Licor; catalog numbers 926-32213 and 026-68072, respectively) were used to clearly distinguish between the Munc13-4 and beta-actin bands, and the blots were imaged using a LI-COR Odyssey CLx imaging device using Image Studio Version 4.0 software.

Degranulation assay

Homogenized splenic tissue was passed through a 70 μm filter, washed with phosphate-buffered saline containing 5% FBS, and plated at 300,000 cells/FACS tube in RPMI containing 10% FBS and 1% penicillin and streptavidin and supplemented with mouse IL-2 (10 ng/mL, 575402; BioLegend). Cells were then incubated for 30 minutes in either the presence or absence of 3 μg/mL of CD3 (Clone 145-2C11, 100301; BioLegend) and 1 μg/mL of CD28 antibody (Clone 37.51, 102101; BioLegend) to produce ''stimulated'' and ''unstimulated'' sample groups, respectively. Subsequently, monensin (420701; BioLegend) and CD107a antibody (BV421, 121617; BD Biosciences) were added to all the cultures, and the cells were incubated for an additional 8 h. Staining for analysis consisted of a live dead cell stain, CD8 (PE,108739; BioLegend), CD44 (UV379, 740215; BD Biosciences), and CD69 (FITC, 557392; BD Biosciences). The chimeric transplant studies also incorporated the use of CD45.1 and CD45.2 antibodies (PerCP-Cy5.5, 560580, BD Biosciences; and BUV737, 564880, BD Biosciences, respectively) to distinguish between cells derived from *Jinx* and CD45.1 engrafted Sca-1 cells.

Cytotoxicity assay

Frozen PBMCs from an FHL3 patient were thawed and stimulated using CD3 and CD28 (7 and 0.5 μg/mL, respectively) for 24 h. These cells were subsequently double transduced with an MOI of 10 for both TPO-CAR and *UNC13D* LV vectors according to the aforementioned transduction protocol. Five days after transduction, these cells were coincubated with M-07e cells. Cell killing was assessed by flow cytometry by looking for cell death markers Annexin V and propidium iodide (PI).

Primary cell and cell lines

Healthy donor T cells were isolated by negative selection from donor PBMC sourced from leukoreduction filters, as previously described.[46,47] The following cell lines were used in this study: NIH 3T3 cells (ATCC number CRL-1658), Jurkat clone E6-1 cells (ATCC number TIB-152), M-07e cells (ACC 104). Munc13-4-deficient T cells were isolated from FHL3 patients treated in the Children's Healthcare of Atlanta (CHOA), Emory University School of Medicine (Atlanta, GA). The patient had biallelic genetic defects: a c.551G>A (p.Trp184*) mutation on one allele and a 253 kb inversion on the other allele. The result was a lack of Munc13-4 protein forma-

tion. Informed consent and IRB approval were obtained for all studies involving human samples.

Cell culture

The following reagents were used for cell culture: DMEM (10-017-CV; Corning), RPMI (10-040-CV; Corning), StemPro (10640-019; Gibco), FBS (S11150H; Atlanta Biologicals), and penicillin/streptomycin (09-757F; Lonza).

Flow cytometry

The following reagents were used throughout the various flow cytometry-based experiments: eFluor 780 viability staining (65-0865-14; ThermoFisher), PE mCD8 (108739; BioLegend), UV379 mCD44 (740215; BD Biosciences), FITC mCD69 antibody (557392; BD Biosciences), BV421 mCD107a (121617; BD Biosciences), PerCP-Cy5.5 CD45.1 (560580; BD Biosciences), BUV737 CD45.2 (564880; BD Biosciences), Annexin V, and PI.

Statistical analysis

All statistical tests were performed using GraphPad Prism version 8.

RESULTS

Stable expression of Munc13-4 in healthy donor cells

To design an optimal LV-based expression system, we set out to assess the dynamic change in the expression of degranulation proteins at baseline and immune activation. Western blot was performed on PBMCs from healthy donors to assess the expression of perforin, Munc13-4, Rab27a, and STXBP2 before and 120 h after stimulation with CD3/CD28 beads (Fig. 1A–C). The results indicate that perforin was upregulated ~20-fold from its baseline levels in response to stimulation and activation, but that Munc13-4, Rab27a, and STXBP2 protein levels were either not significantly different from baseline (Munc13-4 and STXBP2) or only twofold increased from baseline (Rab27a). This suggests that a constitutive promotor driven LV expression system would be appropriate for correcting FHL3-related degranulation defects.

Transduction of FHL3 patient T cells

A LV construct that expresses the cDNA product from the human *UNC13D* gene (GenBank accession number AJ578444.1) under the control of the Ef1α promoter was designed (Fig. 2A). Stimulated PBMCs from an FHL3 patient were transduced using a standard polybrene transduction protocol, and it was observed that these transduced cells expressed Munc13-4 (Fig. 1D). Stimulation of the transduced cells with CD3 and CD28 induced increased expression of the exocytosis marker CD107a (LAMP-1) at the plasma membrane compared with nontransduced patient cells, indicating functionality of the transgenic Munc13-4 (Fig. 1E and Supplementary Fig. S1). The patient's T cells used in this study were naive to EBV; hence, we could not assess cytotoxicity against EBV-transformed lymphoblastoid cell lines. To assess the cytotoxic abilities of the transduced cells, we double transduced FHL3 patient PBMCs with both the *UNC13D* construct and a human thrombopoietin (TPO) chimeric antigen receptor (CAR) construct. This subsequently rendered the double-transduced cells cytotoxically competent and able to recognize cells expressing TPO receptor (MPL). A cytotoxicity assay performed by coculturing these cells with MPL expressing target cells (M-07e cells) demonstrated an increase in cytotoxic function in transduced patient cells compared with nontransduced patient cells (Fig. 1F and Supplementary Fig. S2).

Optimization of the LV construct

To determine the optimal expression system for Munc13-4, several alternative LV vectors were designed (Fig. 2A). Starting with the previously described construct, we added the sequence for green fluorescent protein to act as a marker for transduced cells. Second, we replaced the Ef1α promoter with the synthetic MND promoter that was adapted from Moloney murine leukemia virus and myeloproliferative sarcoma virus elements.[48] Third, we included a Kozak sequence in some of our constructs to enhance translation of transgene mRNA.[49] Finally, we created a codon optimized version of the canonical *UNC13D* transgene using the optimization strategy we previously described.[50] All cloned plasmids were checked for their accuracy using restriction digests and DNA sequencing.

The cloned plasmids were integrated into a four-plasmid transfection system to generate VSV-G pseudotyped LV vectors. Previous FHL3 gene therapy studies found that H/F pseudotyped vectors produced efficient transduction of T cells from FHL3 patients.[22,24] We chose to pseudotype our LV vectors with VSV-G because VSV-

Figure 1. (A) Frozen PBMCs from three HDs were thawed and cultured for 5 days in interleukin 2 supplemented media. Western blot was performed on lysates from these cells before and 5 days after stimulation with CD3 and CD28 beads. The blot was probed for proteins used in cytotoxic degranulation: perforin, Munc13-4, STXBP2, and Rab27a. Beta-actin was used as a loading control. Fold changes from baseline protein expression were calculated **(B)** and change relative to beta-actin **(C)**. **(D)** PBMCs from an FHL3 patient were transduced using the *UNC13D* lentiviral construct, and subsequent Munc13-4 expression levels were assessed by western blot 5 days after transduction. **(E)** Stimulation of these cells using CD3 and CD28 antibody for 4 h induced higher surface expression of CD107a (Lamp-1) in transduced patient cells compared with nontransduced patient cells. **(F)** Viability of target cells (M-07e), non-transduced, single- (*UNC13D*), and double-transduced FHL3 patient T (*UNC13D* and *TPO-CAR*) cells are given in the *top panel*. The *bottom panel* represents the viability of target M-07e cells when cocultured with different effector T cells (untransduced FHL3 T cells, *UNC13D* transduced FHL3 T cells, *UNC13D* and *TPO-CAR* transduced FHL3 T cells, and *TPO-CAR* transduced HD T cells). Viability assessed by PI and Annexin V staining. (*Significance level of $p \leq 0.05$.) FHL3, familial hemophagocytic lymphohistiocytosis type 3; HDs, healthy donors; PI, propidium iodide.

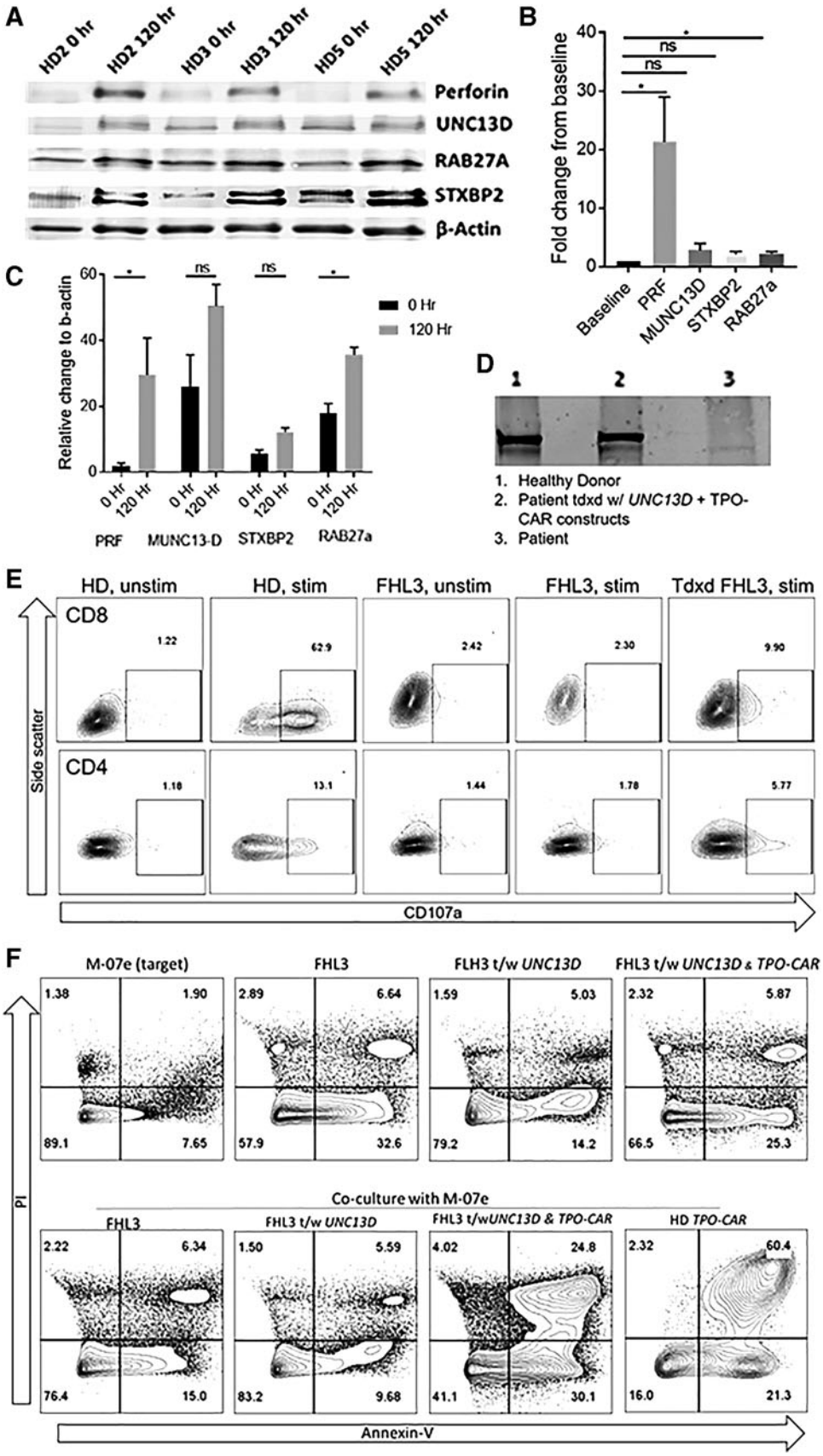
A
HD2 0 hr
HD2 120 hr
HD3 0 hr
HD3 120 hr
HD5 0 hr
HD5 120 hr
Perforin
UNC13D
RAB27A
STXBP2
β-Actin
B
Fold change from baseline
ns
ns
Baseline
PRF
MUNC13D
STXBP2
RAB27a
C
Relative change to b-actin
0 Hr
120 Hr
PRF
MUNC13-D
STXBP2
RAB27a
D
1
2
3
1. Healthy Donor
2. Patient tdxd w/ UNC13D + TPO-CAR constructs
3. Patient
E
HD, unstim
HD, stim
FHL3, unstim
FHL3, stim
Tdxd FHL3, stim
CD8
CD4
Side scatter
CD107a
F
M-07e (target)
FHL3
FLH3 t/w UNC13D
FHL3 t/w UNC13D & TPO-CAR
PI
Co-culture with M-07e
FHL3
FHL3 t/w UNC13D
FHL3 t/wUNC13D & TPO-CAR
HD TPO-CAR
Annexin-V

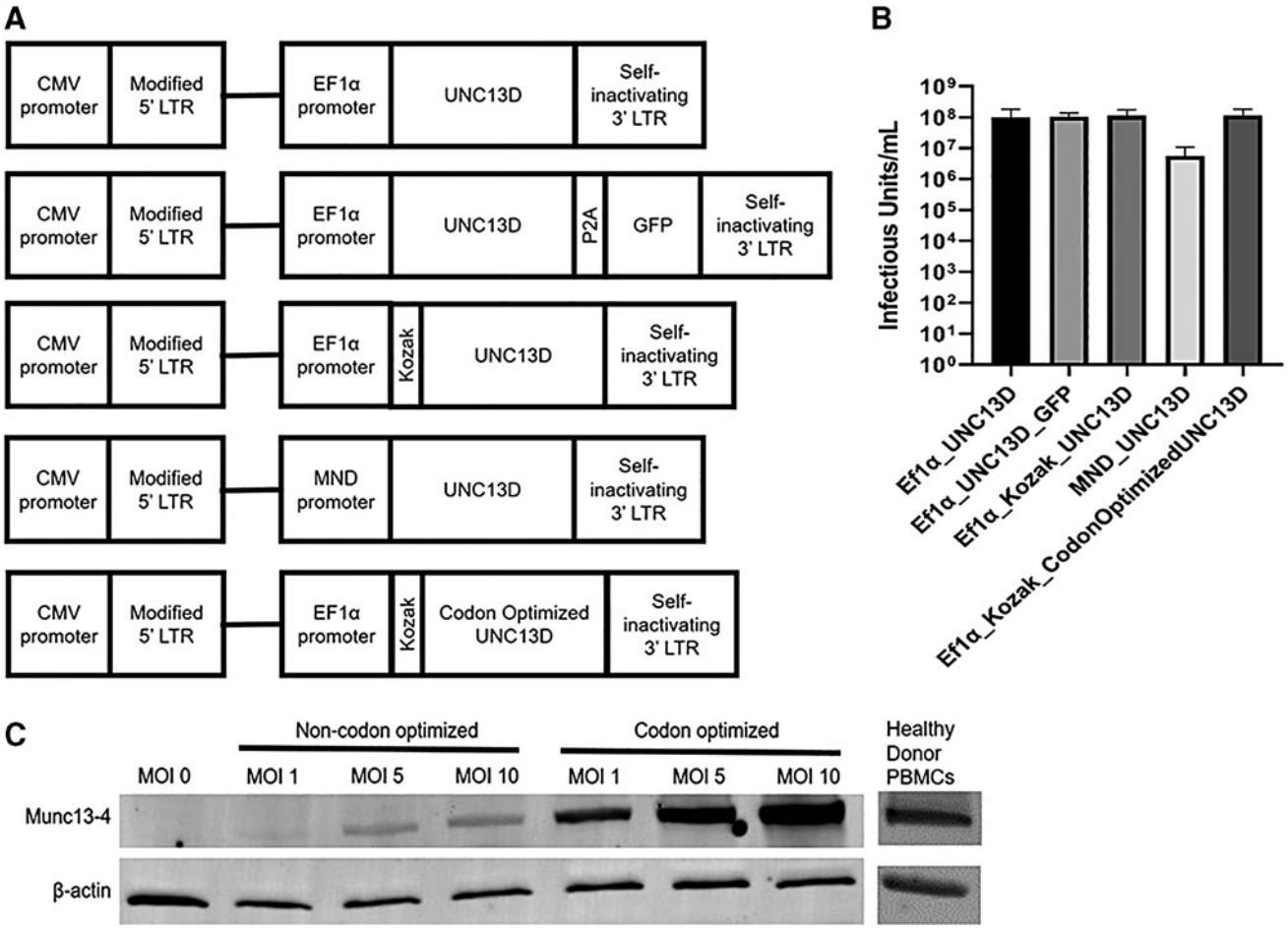

Figure 2. **(A)** Diagram of the described lentiviral vector constructs. **(B)** Modification to the original lentiviral construct did not produce any change in viral titer as assessed by transduction of HEK 293T cells (Kruskal–Wallis H-test, $p=0.48$). **(C)** Versions of the lentiviral construct that were under the control of the Ef1α promoter and included a Kozak sequence demonstrated that the codon-optimized version of the *UNC13D* gene is expressed more highly in NIH 3T3 cells than the noncodon-optimized version of the gene. At MOIs of 5 and 10, the level of Munc13-4 expression exceeded physiological expression levels of Munc13-4 in PBMCs from a HD. VCNs for the noncodon optimized and codon optimized versions of the construct were, respectively, 0.22 and 0.18 at an MOI of 10. VCNs, viral copy numbers.

G is pantropic,[51] and clinical trials using VSV-G pseudotyped LV vectors are underway (NCT02234934, NCT01560182, NCT03315078, NCT02333760, and NCT03818763[52,53]). Also, we were concerned about the findings from some studies that have shown that H/F pseudotyped LV vectors can induce syncytia formation in transfected cells, leading to cell death and subsequent low titers.[54,55] In addition, it has been shown that H/F pseudotyped LV vectors have difficulty targeting murine cells,[56] and also that native-form H protein induces a humoral immune response in measles-vaccinated individuals, which can lead to neutralization and clearance of H/F pseudotyped LV vectors.[57]

We were reliably able to produce these self-inactivating LV vectors at similar titers (Fig. 2B) using our previously described HEK 293T transfection protocol.[58] We demonstrated that these vectors could be used to transduce NIH 3T3 cells (a mouse embryonic fibroblast cell line that does not express Munc13-4) and robustly express Munc13-4 protein. We achieved higher levels of protein expression from cells that were transduced with the Ef1α_Kozak_Codon-Optimized-*UNC13D* construct (Fig. 2C), and therefore we chose to confine our subsequent transduction experiments to use this particular LV construct.

Identifying potentially therapeutic Munc13-4 expression levels

Jinx mice were irradiated twice with 550 rads of gamma radiation and transplanted with different mixtures of *Jinx* whole bone marrow ($CD45.2^+$) and wild-type (WT) bone marrow ($CD45.1^+$). Flow cytometry analysis showed that 6 weeks after transplantation both WT and *Jinx* bone marrow engrafted in the recipient mice in proportions consistent with the original transplant. Furthermore, the ratios of CD45.2 to CD45.1 positive cell remained consistent across specific $CD8^+$, $CD4^+$, and $NK1.1^+$ cell subpopulations (Fig. 3). At baseline, we established that following LCMV infection, there was a robust increase in $CD44^+$ CD8 T cells, and this memory response was comparable between WT and Jinx mice (Fig. 4A–E). Twenty-two weeks post-transplantation, the mice were killed and their splenocytes

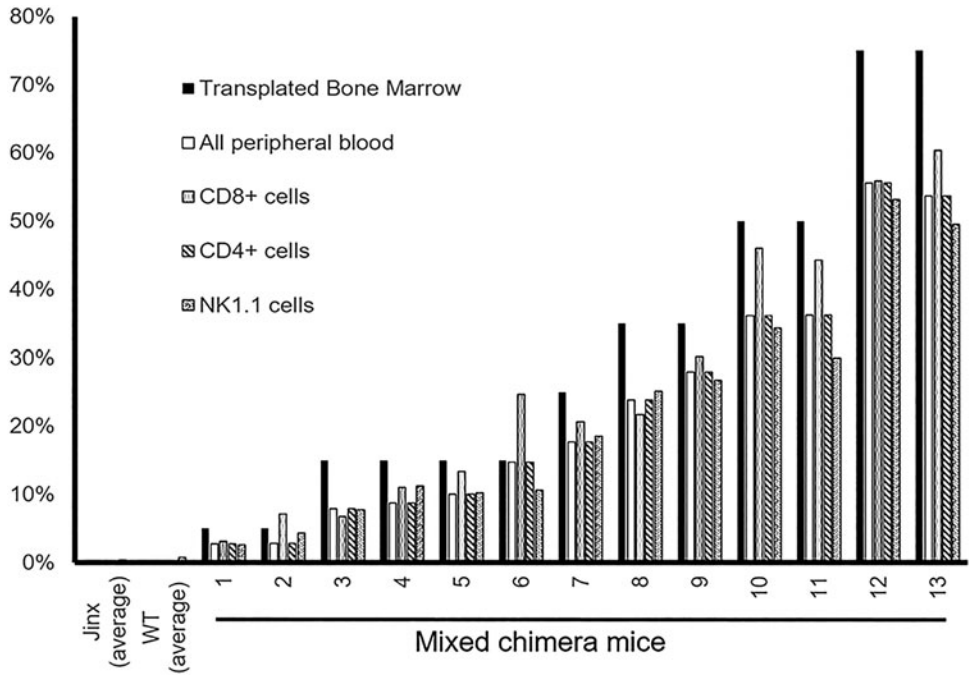

Figure 3. Six weeks after transplant, flow cytometry analysis indicated that the chimerically transplanted mice maintained their chimerism within the bulk peripheral blood and also across the $CD8^+$, $CD4^+$, and $NK1.1^+$ cell populations.

were stimulated with CD3 and CD28 free antibody and analyzed for the expression of plasma membrane-bound CD107a (Lamp-1) and CD69. $CD8^+$, and $CD44^+$ cells from the mice transplanted with WT $CD45.1^+$ bone marrow degranulated similarly to those from nontransplanted WT mice, indicating that HSCT did not affect degranulation capacity (Fig. 4E). Consistent with previous research, splenocytes from WT, *Jinx*, and chimeric mice all increased CD69 expression after stimulation (Fig. 4G), corroborating the evidence that the presence or absence of Munc13-4 expression does not affect the mechanism of T cell activation.[59] Mice with 15% of $CD45.1^+$ mouse bone marrow showed CD107a upregulation comparable with that of a WT mouse (Fig. 4F). Together, these data show that similar to studies carried out in the FHL2 gene therapy mouse model,[60] a 15% correction might be sufficient to recapitulate the WT degranulation phenotype in FHL3 disease model mice.

Gene transfer into the FHL3 disease mouse model

To determine the *in vivo* efficacy of our gene therapy approach within the FHL3 mouse model, Sca-1 cells were isolated from donor *Jinx* mice and transduced with the Ef1α_Kozak_CodonOptimized*UNC13D* LV vector. Subsequently, one million of these cells were transplanted into *Jinx* mouse recipients according to our previously published protocols (Fig. 5A).[61] Within 12 weeks, the mice had normal complete blood counts (CBCs) (Fig. 5B) and an average copy number of 0.15 in the peripheral blood. Twenty weeks after transplantation, the mice were infected with 2×10^5 PFU LCMV Armstrong to induce the FHL3 disease phenotype.[59] Ten days after infection, the mice were killed, and degranulation assay results ascertained a statistically significant increase in CD107a expression in stimulated cells from gene therapy-modified mice compared with nontransplanted *Jinx* mice (Fig. 5C,

Figure 4. (A) Flow gating strategy. **(B, C)** WT mice that were infected with either one or two doses of LCMV Armstrong infection (2×10^5 PFU/mouse) developed greater numbers of $CD44^+$ $CD8^+$ cells in an antiviral immune response compared with LCMV-naive mice (unpaired *t*-test, $p=0.04$ and 0.02 for naive to primary and naive to secondary infections, respectively). **(D)** WT and *Jinx* mice do not differ in their increase in the number of $CD8^+$ $CD44^+$ cells as a result of a single 2×10^5 PFU/mouse infection of LCMV Armstrong (unpaired *t*-test, $p=0.396$). **(E)** $CD8^+$ $CD44^+$ splenocytes from nontransplanted C57BL/6 mice and the $CD45.1^+$ engrafted cells from chimerically transplanted *Jinx* mice showed similar levels of CD69 and CD107a expression before (*gray*) and after (*black*) stimulation with CD3 and CD28 antibodies. (Mann–Whitney test, $p=0.2253$ for CD69 expression, $p=0.8846$ for CD107a expression.) **(F, G)** Twenty weeks after transplantation, the chimerically transplanted mice were infected intraperitoneally with 2×10^5 PFU LCMV Armstrong to recapitulate the FHL3 disease model. Eight days after infection, the mice were killed, and their $CD44^+$ $CD8^+$ splenocytes were assessed for the ability to activate **(G**, Spearman's rank-order correlation, two-tailed: $r=0.2105$, $p=0.508$**)** and degranulate **(F**, Spearman's rank-order correlation, two-tailed: $r=0.814$, $p=0.002$**)** compared with the $CD44^+$ $CD8^+$ splenocytes from LCMV-infected WT and *Jinx* mice. The data points labeled as *Jinx* and "WT" mice represent the results obtained from nontransplanted control mice, and all other data represent chimerically transplanted mice.

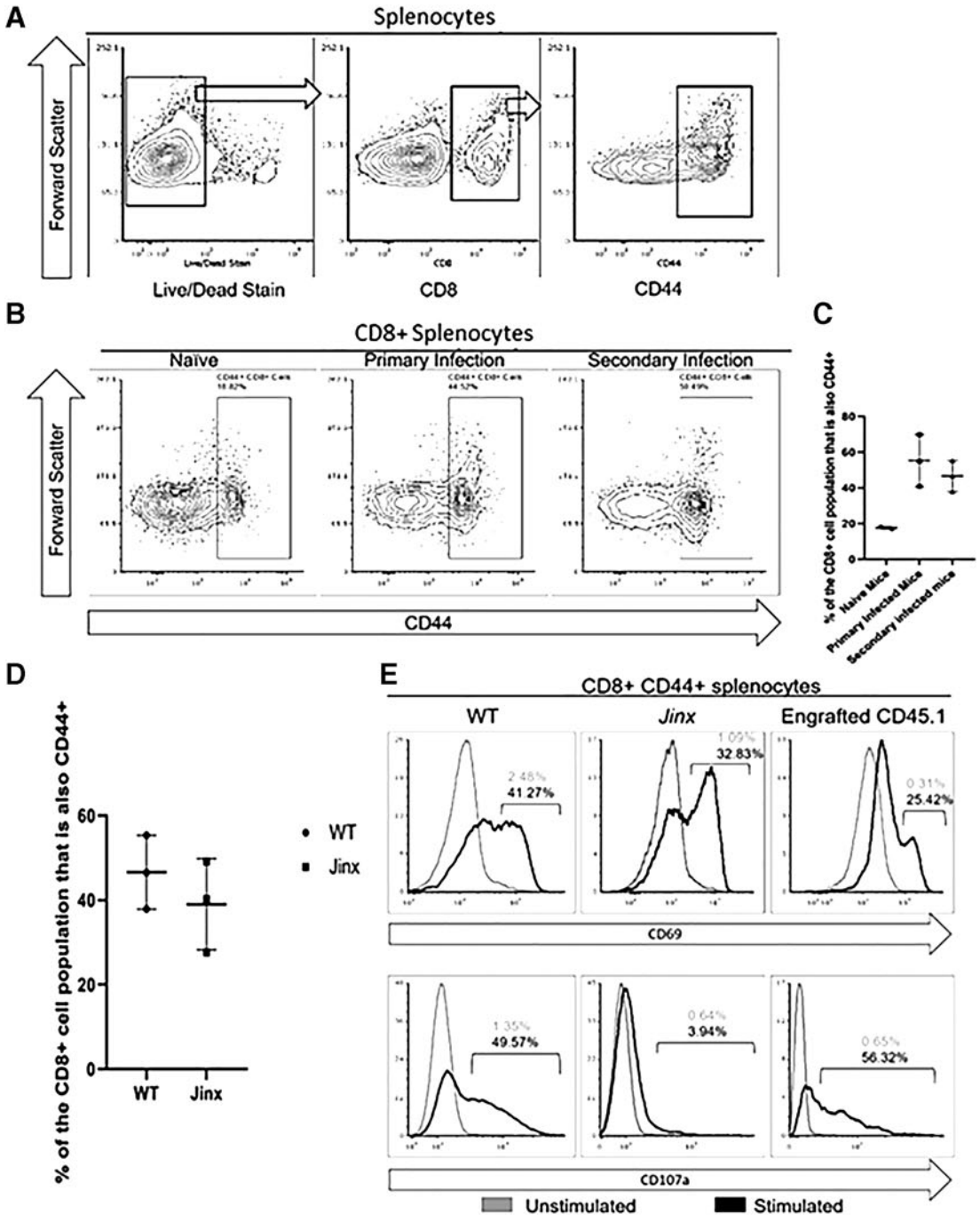
A
Splenocytes
Forward Scatter
Live/Dead Stain
CD8
CD44
B
CD8+ Splenocytes
Naïve
Primary Infection
Secondary Infection
Forward Scatter
CD44
C
% of the CD8+ cell population that is also CD44+
Naive Mice
Primary Infected Mice
Secondary infected mice
D
% of the CD8+ cell population that is also CD44+
WT
Jinx
E
CD8+ CD44+ splenocytes
WT
Jinx
Engrafted CD45.1
2.48%
41.27%
1.09%
32.83%
0.31%
25.42%
CD69
1.35%
49.57%
0.64%
3.94%
0.65%
56.32%
CD107a
Unstimulated
Stimulated
F
Increase in CD107a gated cells (%)
% CD45.1 Chimerism
WT
WT
Jinx
Jinx
G
Increase in CD69 gated cells (%)
% CD45.1 Chimerism
Jinx
WT
WT
Jinx

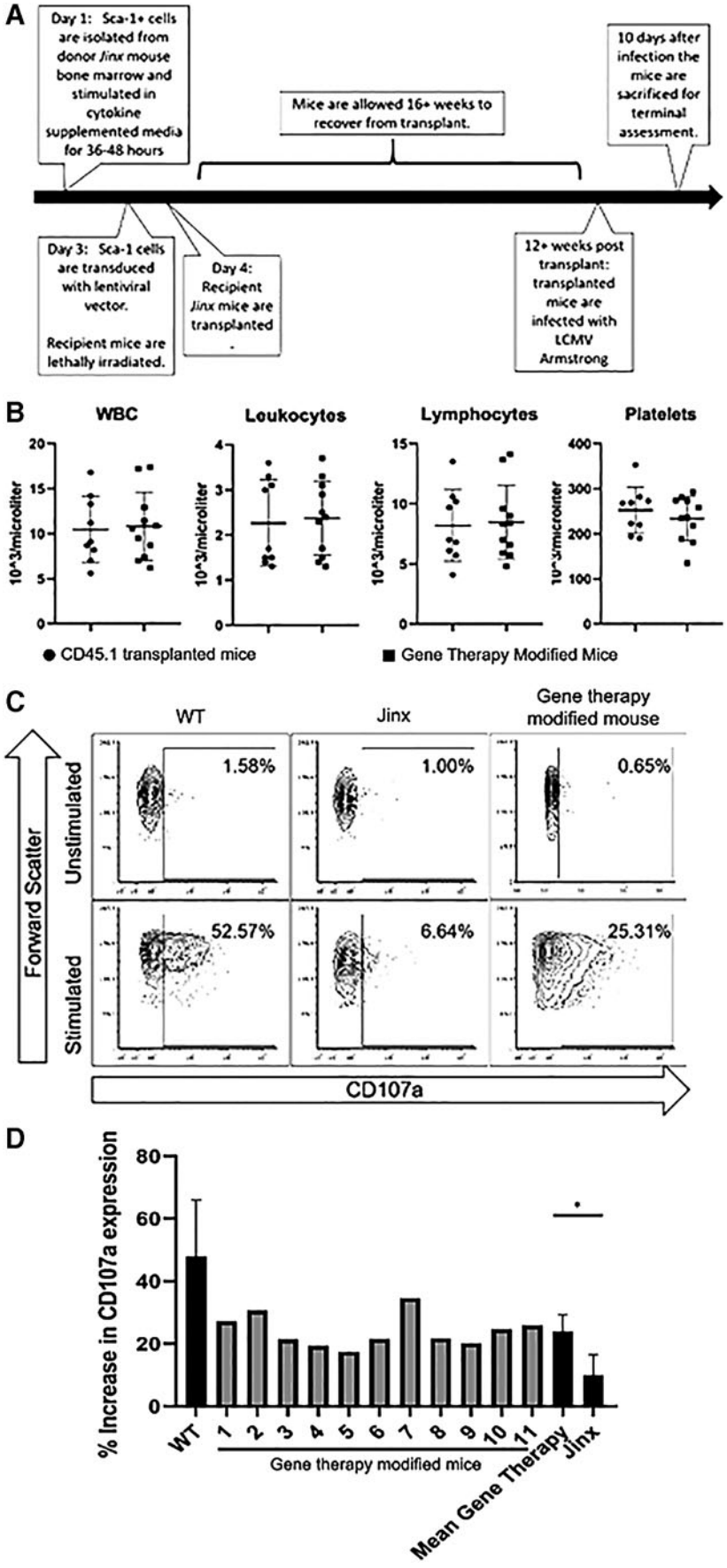

Figure 5. **(A)** Diagram of experimental layout. **(B)** After 12 weeks of transplantation, CBCs showed no difference between gene therapy-modified mice and mice that were transplanted with CD45.1 Sca-1 cells in the WBC, leukocyte, and lymphocyte populations (unpaired, two-tailed *t*-test, $p = 0.82$, 0.84, 0.79, and 0.42 for WBCs, leukocytes, lymphocytes, and platelets, respectively). **(C, D)** Gene therapy-modified mice showed significantly greater upregulation of surface CD107a after stimulation with CD3/CD28 antibody (two-tailed Mann–Whitney *U*-test, $p = 0.005$). CBC, complete blood count; WBC, white blood cell.

D). The mean viral copy number (VCN) in the bulk splenocyte population was 0.30 copies per cell. Despite LCMV challenge, we did not observe an obvious HLH phenotype in our *Jinx* mice.

DISCUSSION

Current treatment for HLH entails an allogeneic HSCT, but the success of this procedure is greatly influenced by the ability to control disease-related inflammation before transplantation and the availability of HLA-matched HSCT donors. Inadequate inflammation control increases the risk of a patient experiencing transplant-related mortality, usually caused by infections, veno-occlusive disease, pneumonitis, graft failure, and/or graft-versus-host disease.[62] Only 53% of HLH patients achieve full resolution of their inflammation before HSCT, and of these patients, 13% experience disease reactivation.[9] Furthermore, the inability to control inflammation before HSCT accounts for 22% of diagnosed HLH patients dying before HSCT.[9] In light of suboptimal outcomes, we and others have proposed a gene therapy treatment by which a patient's T cells would be isolated, transduced with a corrective construct, and transfused back into the patient such that the transduced cells could resolve the cause of inflammation and if necessary, allow for additional HSPC-based autologous gene therapy or allogeneic HSCT.[22,24]

LV gene therapy utilizing a constitutive promoter is better suited for genetic defects where the protein is consistently expressed without much dynamic change upon activation. Our results showed limited to no significant change in expression levels of degranulation proteins Munc13-4, STXBP2, and Rab27a after TCR stimulation. Thus, these genetic defects are ideal candidates for constitutively expressing LV-based gene therapy strategies. In contrast, perforin seems to be dynamically regulated, and therefore gene therapy for perforin deficiency will likely necessitate the use of a perforin-specific promoter as described in previous studies[3,63] or maybe a better candidate for gene editing rather than gene addition strategies.

We were able to successfully augment Munc13-4 expression in activated patient T cells, and restores *in vitro* degranulation. We note that our results corroborate those from other studies that have shown that T cells from FHL3 patients, despite having been subjected to a hyperinflammatory environment and massive *in vivo* expansion, are permissive to LV transduction.[22,24,64] Furthermore, using a dual transduction protocol we were able to restore cytotoxic capacity in FHL3 T cells, demonstrating the effectiveness of our LV vector and the potential of a dual *UNC13D* and CAR-T transduction protocol as a therapeutic option to reduce viral-induced inflammation before a patient received HSCT.

Recent reports showed that human T cells and mouse hematopoietic stem cells can be transduced with LV vectors that express a codon-optimized *UNC13D* cDNA under the control of the Ef1a or EFS promoters.[22,23] These cells achieved VCNs of 2^{24} and 5 copies per cell after transduction using MOIs of 100.[22–24] Scaling LV production to be able to produce such large quantities of LVs for treating a patient remains a major challenge for the field of gene therapy, and so we created multiple LV constructs with the intent of producing a superior and scalable vector. Each construct was reliably and efficiently produced, but transduction into cell lines and subsequent western blot analysis showed that the codon-optimized version produced the highest expression of Munc13-4, which was comparable with constitutive expression levels in human PBMCs, even at relatively low MOIs.

Studies of HLH patients that received HSCT reported that between 20% and 30% bone marrow chimerism is protective against disease reactivation, although the correlation between donor chimerism and patient outcome is by no means perfect.[65] Similarly, gene therapy studies in the perforin-deficient FHL2 mouse model showed that as little as 10–20% engraftment of WT cells within the bone marrow of transplanted mice was sufficient to restore immune function.[60] We sought to determine what percent correction in a Munc13-4 null mouse model (*Jinx* mouse model) would be sufficient to correct the Munc13-4-deficient degranulation defect. To this end, varying donor chimerism was established in *Jinx* mice using WT (CD45.1) and *Jinx* (CD45.2) bone marrow. As expected, positive correlation was noted between the proportion of engrafted CD45.1 cells and degranulation capacity. No correlation was observed between the proportion of engrafted CD45.1 cells and cell activation as assessed by cell surface CD69 expression. This is because Munc13-4 deficiency does not interfere with immune activation and T cell from *Jinx* mice are capable of immune activation. Although the overall trends of this experiment are not surprising, what is important is the proportion of degranulation in 15% WT mixed chimera mice is comparable with that of WT mice. This result is consistent with clinical data,[65] and the finding that engraftment of 10–20% WT bone marrow in perforin$^{-/-}$ mice was enough to reduce serum levels of interferon γ (IFN-γ) after LCMV infection,[60] and that a perforin$^{-/-}$ mouse with as little as 8–15% of gene therapy-modified CD8 T cells or >30% gene therapy-modified HSCs is protective against LCMV.[63,66] Although it would be an overreach to definitely say at this point that FHL3 gene therapy requires a minimum of 15% degranulation competent T cell compartment, the existing body of evidence suggests that even a smaller subset of immunocompetent cells can compensate and adequately regulate the immune system. Further *in vivo* studies are needed to definitely determine the threshold needed for disease phenotype correction.

There were some concerns if the constitutional expression of Munc13-4 in HSPC could impair engraftment. We noted robust engraftment of *UNC13D* gene-transduced HSPC. By 12 weeks post-transplantation, these mice had

normal complete blood counts compared with control *Jinx* mice that had received one million CD45.1 Sca-1 cells. This indicates that *UNC13D* gene therapy modification does not negatively affect engraftment potential.

Twenty weeks after transplantation, mice were injected with LCMV Armstrong to induce the FHL3 disease phenotype.[59] For our degranulation assays, we specifically observed changes in CD107a expression within the memory CD8 T cell population ($CD44^+$ and $CD8^+$ cells). Upon stimulation, these cells showed significantly higher expression of CD107a compared with nonmodified LCMV-infected *Jinx* mice. Although an improvement, CD107a upregulation was less than that observed in WT mice, perhaps as a result of transgene integration into transcriptionally inactive genome sites and low copy number achieved. CD107a expression on cytotoxic cells is an indicator of the restoration of cytolytic ability.[67] Therefore, the restoration of CD107a expression in our degranulation assays indicates successful gene therapy modification and potential for FHL3 disease correction.

It is worth noting that a more clinically relevant gene therapy model would involve first inducing illness in *Jinx* mice through LCMV infection and then correcting it with HSPC-based gene therapy. Furthermore, comparing the work presented here with previous FHL3 gene therapy mouse studies may be difficult owing to how we elected to infect our mice with LCMV Armstrong rather than the more virulent WE strain of LCMV, which was used in previous FHL3 gene therapy studies and produces a more clinically robust disease model.[23] The LCMV Armstrong strain was used because of the well-described CD8 T cell response in *Jinx* mice.[59,68] Indeed, we were able to recapitulate previous findings showing a robust CD8 T cell memory response upon LCMV Armstrong infection, and gene therapy improved degranulation of these cells. However, despite the *Jinx* mice having a fixed degranulation defect, we could not adequately model human FHL3 disease utilizing less virulent LCMV Armstrong strain as an infection trigger. Future studies with either a higher dose of LCMV Armstrong or the use of more virulent WE strain of LCMV or use of a different infectious trigger could better recapitulate features of human FHL3 such as cytopenia, elevated liver enzymes, elevated IFN-γ, sIL2R, and ferritin. Once this is achieved, it will help in the assessment of *in vivo* disease activity and laboratory parameters correction after HSC-based gene therapy. Also, additional studies such as lineage-specific VCN analysis, deeper immunophenotyping, viral clearance, integration site analysis, and secondary transplant studies could give valuable preclinical data critical for initiating gene therapy studies for FHL3 in humans.

Overall, an *UNC13D* LV vector was optimized to effectively modify FHL3 patient T cells and hematopoietic stem cells from the FHL3 (*Jinx*) mice. Furthermore, we showed that having 15% degranulation-competent cells is still sufficient to produce degranulation response comparable with WT. Therefore, a significant body of preclinical data supports the pursuit of autologous HSCT or T cell LV vector gene therapy as a transformative approach to FHL3 disease management or cure.

ACKNOWLEDGMENTS

Stocks of LCMV Armstrong were generously supplied by Dr. Rafi Ahmed Lab.

AUTHOR DISCLOSURE

The authors declare no conflict of interest.

FUNDING INFORMATION

NHLBI 1K08HL141635-01A1, Atlanta Pediatric Scholars Program K12 Scholar supported by grant K12HD072245 and U54AI082973.

SUPPLEMENTARY MATERIAL

Supplementary Figure S1
Supplementary Figure S2

REFERENCES

1. Henter JI, Elinder G, Ost A. Diagnostic guidelines for hemophagocytic lymphohistiocytosis. The FHL Study Group of the Histiocyte Society. Semin Oncol 1991;18:29–33.

2. Henter JI, Horne A, Arico M, et al. HLH-2004: diagnostic and therapeutic guidelines for hemophagocytic lymphohistiocytosis. Pediatr Blood Cancer 2007;48:124–131.

3. Das R, Bar N, Ferreira M, et al. Early B cell changes predict autoimmunity following combination immune checkpoint blockade. J Clin Invest 2018;128:715–720.

4. Filipovich AH. Hemophagocytic lymphohistiocytosis (HLH) and related disorders. Hematology Am Soc Hematol Educ Program 2009:127–131.

5. Vick EJ, Patel K, Prouet P, et al. Proliferation through activation: hemophagocytic lymphohistiocytosis in hematologic malignancy. Blood Adv 2017;1:779–791.

6. Eife R, Janka GE, Belohradsky BH, et al. Natural killer cell function and interferon production in familial hemophagocytic lymphohistiocytosis. Pediatr Hematol Oncol 1989;6:265–272.

7. Kim T, Kulick CG, Kortepeter CM, et al. Hemophagocytic lymphohistiocytosis associated with the use of lamotrigine. Neurology 2019;92:e2401–e2405.

8. Feldmann J, Callebaut I, Raposo G, et al. Munc13-4 is essential for cytolytic granules fusion and is mutated in a form of familial hemophagocytic lymphohistiocytosis (FHL3). Cell 2003;115:461–473.

9. Henter JI, Samuelsson-Horne A, Arico M, et al. Treatment of hemophagocytic lymphohistiocytosis with HLH-94 immunochemotherapy and bone

marrow transplantation. Blood 2002;100:2367–2373.

10. Ouachee-Chardin M, Elie C, de Saint Basile G, et al. Hematopoietic stem cell transplantation in hemophagocytic lymphohistiocytosis: a single-center report of 48 patients. Pediatrics 2006;117: e743–e750.

11. Baker KS, DeLaat CA, Steinbuch M, et al. Successful correction of hemophagocytic lymphohistiocytosis with related or unrelated bone marrow transplantation. Blood 1997;89:3857–3863.

12. Horne A, Janka G, Maarten Egeler R, et al. Haematopoietic stem cell transplantation in haemophagocytic lymphohistiocytosis. Br J Haematol 2005;129:622–630.

13. Imashuku S, Hibi S, Todo S, et al. Allogenic hematopoietic stem cell transplanation for patients with hemophagocytic syndrome (HPS) in Japan. Bone Marrow Transplant 1999;23:569–572.

14. Cesaro S, Locatelli F, Lanino E, et al. Hematopoietic stem cell transplantation for hemophagocytic lymphohistiocytosis: a retrospective analysis of data from the Italian Association of Pediatric Hematology Oncology (AIEOP). Haematologica 2008;93:1694–1701.

15. Durken M, Horstmann M, Bieling P, et al. Improved outcome in haemophagocytic lymphohistiocytosis after bone marrow transplantation from related and unrelated donors: a single-centre experience of 12 patients. Br J Haematol 1999;106: 1052–1058.

16. Cooper N, Rao K, Gilmour K, et al. Stem cell transplantation with reduced-intensity conditioning for hemophagocytic lymphohistiocytosis. Blood 2006;107:1233–1236.

17. Cooper N, Rao K, Goulden N, et al. The use of reduced-intensity stem cell transplantation in haemophagocytic lymphohistiocytosis and Langerhans cell histiocytosis. Bone Marrow Transplant 2008;42(Suppl 2):S47–S50.

18. Bergsten E, Horne A, Arico M, et al. Confirmed efficacy of etoposide and dexamethasone in HLH treatment: long term results of the cooperative HLH-2004 study. Blood 2017;130:2728–2738.

19. Malinowska I, Machaczka M, Popko K, et al. Hemophagocytic syndrome in children and adults. Arch Immunol Ther Exp (Warsz) 2014;62:385–394.

20. Allen CE, Marsh R, Dawson P, et al. Reduced-intensity conditioning for hematopoietic cell transplant for HLH and primary immune deficiencies. Blood 2018;132:1438–1451.

21. Trottestam H, Horne A, Arico M, et al. Chemoimmunotherapy for hemophagocytic lymphohistiocytosis: long-term results of the HLH-94 treatment protocol. Blood 2011;118:4577–4584.

22. Dettmer V, Bloom K, Gross M, et al. Retroviral UNC13D gene transfer restores cytotoxic activity of T cells derived from familial hemophagocytic lymphohistiocytosis type 3 patients in vitro. Hum Gene Ther 2019;30:975–984.

23. Soheili T, Durand A, Sepulveda FE, et al. Gene transfer into hematopoietic stem cells reduces HLH manifestations in a murine model of Munc13-4 deficiency. Blood Adv 2017;1:2781–2789.

24. Soheili T, Riviere J, Ricciardelli I, et al. Gene-corrected human Munc13-4-deficient $CD8^+$ T cells can efficiently restrict EBV-driven lymphoproliferation in immunodeficient mice. Blood 2016;128: 2859–2862.

25. Ammann S, Lehmberg K, Zur Stadt U, et al. Effective immunological guidance of genetic analyses including exome sequencing in patients evaluated for hemophagocytic lymphohistiocytosis. J Clin Immunol 2017;37:770–780.

26. Jordan MB, Allen CE, Weitzman S, et al. How I treat hemophagocytic lymphohistiocytosis. Blood 2011;118:4041–4052.

27. Meeths M, Chiang SC, Wood SM, et al. Familial hemophagocytic lymphohistiocytosis type 3 (FHL3) caused by deep intronic mutation and inversion in UNC13D. Blood 2011;118:5783–5793.

28. Seo JY, Song JS, Lee KO, et al. Founder effects in two predominant intronic mutations of UNC13D, c.118-308C>T and c.754-1G>C underlie the unusual predominance of type 3 familial hemophagocytic lymphohistiocytosis (FHL3) in Korea. Ann Hematol 2013;92:357–364.

29. Elstak ED, te Loo M, Tesselaar K, et al. A novel Dutch mutation in UNC13D reveals an essential role of the C2B domain in munc13-4 function. Pediatr Blood Cancer 2012;58:598–605.

30. Chen Z, Cooper B, Kalla S, et al. The Munc13 proteins differentially regulate readily releasable pool dynamics and calcium-dependent recovery at a central synapse. J Neurosci 2013;33:8336–8351.

31. Zur Stadt U, Beutel K, Kolberg S, et al. Mutation spectrum in children with primary hemophagocytic lymphohistiocytosis: molecular and functional analyses of PRF1, UNC13D, STX11, and RAB27A. Hum Mutat 2006;27:62–68.

32. Entesarian M, Chiang SC, Schlums H, et al. Novel deep intronic and missense UNC13D mutations in familial haemophagocytic lymphohistiocytosis type 3. Br J Haematol 2013;162:415–418.

33. Bin NR, Ma K, Tien CW, et al. C2 domains of Munc13-4 are crucial for Ca(2+)-dependent degranulation and cytotoxicity in NK cells. J Immunol 2018;201:700–713.

34. Pivot-Pajot C, Varoqueaux F, de Saint Basile G, et al. Munc13-4 regulates granule secretion in human neutrophils. J Immunol 2008;180:6786–6797.

35. Xu R, Zhou J, Zhou XD, et al. Munc134 mediates human neutrophil elastaseinduced airway mucin5AC hypersecretion by interacting with syntaxin2. Mol Med Rep 2018;18:1015–1024.

36. Cardenas EI, Breaux K, Da Q, et al. Platelet Munc13-4 regulates hemostasis, thrombosis and airway inflammation. Haematologica 2018;103: 1235–1244.

37. Rodarte EM, Ramos MA, Davalos AJ, et al. Munc13 proteins control regulated exocytosis in mast cells. J Biol Chem 2018;293:345–358.

38. Janka GE. Familial and acquired hemophagocytic lymphohistiocytosis. Annu Rev Med 2012;63:233–246.

39. Giardino G, De Luca M, Cirillo E, et al. Two brothers with atypical UNC13D-related hemophagocytic lymphohistiocytosis characterized by massive lung and brain involvement. Front Immunol 2017;8:1892.

40. Chehab T, Santos NC, Holthenrich A, et al. A novel Munc13-4/S100A10/annexin A2 complex promotes Weibel-Palade body exocytosis in endothelial cells. Mol Biol Cell 2017;28:1688–1700.

41. Gao J, Aksoy BA, Dogrusoz U, et al. Integrative analysis of complex cancer genomics and clinical profiles using the cBioPortal. Sci Signal 2013;6: pl1.

42. Messenger SW, Woo SS, Sun Z, et al. A Ca(2+)-stimulated exosome release pathway in cancer cells is regulated by Munc13-4. J Cell Biol 2018; 217:2877–2890.

43. Brown HC, Zakas PM, George SN, et al. Target-cell-directed bioengineering approaches for gene therapy of hemophilia A. Mol Ther Methods Clin Dev 2018;9:57–69.

44. Johnston JM, Denning G, Doering CB, et al. Generation of an optimized lentiviral vector encoding a high-expression factor VIII transgene for gene therapy of hemophilia A. Gene Ther 2013;20:607–615.

45. Ni D, Xu P, Gallagher S. Immunoblotting and immunodetection. Curr Protoc Protein Sci 2017;88: 10.10.1–10.10.37

46. Wegehaupt AK, Roufs EK, Hewitt CR, et al. Recovery and assessment of leukocytes from LR Express filters. Biologicals 2017;49:15–22.

47. Neron S, Dussault N, Racine C. Whole-blood leukoreduction filters are a source for cryopreserved cells for phenotypic and functional investigations on peripheral blood lymphocytes. Transfusion 2006;46:537–544.

48. Challita PM, Skelton D, el-Khoueiry A, et al. Multiple modifications in cis elements of the long terminal repeat of retroviral vectors lead to increased expression and decreased DNA methylation in embryonic carcinoma cells. J Virol 1995; 69:748–755.

49. Kozak M. Point mutations define a sequence flanking the AUG initiator codon that modulates translation by eukaryotic ribosomes. Cell 1986;44:283–292.

50. Brown HC. Bioengineering viral transgenes for the treatment of hemophilias. Doctoral dissertation, Molecular and Systems Pharmacology. Emory University, 2016. https://etd.library.emory.edu/concern/etds/2z10wq65r?locale=en (last accessed June 6, 2020).

51. Chen Y, Miller WM, Aiyar A. Transduction efficiency of pantropic retroviral vectors is controlled by the envelope plasmid to vector plasmid ratio. Biotechnol Prog 2005;21:274–282.

52. Santilli G, Almarza E, Brendel C, et al. Biochemical correction of X-CGD by a novel chimeric promoter regulating high levels of transgene expression in myeloid cells. Mol Ther 2011;19: 122–132.

53. Brendel C, Rothe M, Santilli G, et al. Non-clinical efficacy and safety studies on G1XCGD, a lentiviral vector for ex vivo gene therapy of X-linked chronic granulomatous disease. Hum Gene Ther Clin Dev 2018;29:69–79.

54. Ozog S, Chen CX, Simpson E, et al. CD46 null packaging cell line improves measles lentiviral vector production and gene delivery to hematopoietic stem and progenitor cells. Mol Ther Methods Clin Dev 2019;13:27–39.

55. Takeuchi K, Miyajima N, Nagata N, et al. Wild-type measles virus induces large syncytium formation in primary human small airway epithelial cells by a SLAM(CD150)-independent mechanism. Virus Res 2003;94:11–16.

56. Delville M, Soheili T, Bellier F, et al. A nontoxic transduction enhancer enables highly efficient lentiviral transduction of primary murine T cells and hematopoietic stem cells. Mol Ther Methods Clin Dev 2018;10:341–347.

57. Levy C, Amirache F, Costa C, et al. Lentiviral vectors displaying modified measles virus gp overcome pre-existing immunity in in vivo-like transduction of human T and B cells. Mol Ther 2012;20:1699–1712.

58. Johnston JM, Denning G, Moot R, et al. High-throughput screening identifies compounds that enhance lentiviral transduction. Gene Ther 2014; 21:1008–1020.

59. Crozat K, Hoebe K, Ugolini S, et al. Jinx, an MCMV susceptibility phenotype caused by disruption of Unc13d: a mouse model of type 3 familial hemophagocytic lymphohistiocytosis. J Exp Med 2007;204:853–863.

60. Terrell CE, Jordan MB. Mixed hematopoietic or T-cell chimerism above a minimal threshold restores perforin-dependent immune regulation in perforin-deficient mice. Blood 2013;122:2618–2621.

61. Tran R, Myers DR, Denning G, et al. Microfluidic transduction harnesses mass transport principles to enhance gene transfer efficiency. Mol Ther 2017;25:2372–2382.

62. Seo JJ. Hematopoietic cell transplantation for hemophagocytic lymphohistiocytosis: recent advances and controversies. Blood Res 2015;50: 131–139.

63. Carmo M, Risma KA, Arumugam P, et al. Perforin gene transfer into hematopoietic stem cells improves immune dysregulation in murine models of perforin deficiency. Mol Ther 2015; 23:737–745.

64. Tayebeh-Shabi Soheili IR, Riviere J, Durand A, et al. Correction of CTLs cytotoxic function defect by SIN-lentiviral mediated expression of Munc13-4 in type 3 familial hemophagocytic lymphohistiocytosiss. American Society of Gene and Cell Therapy Meeting Abstracts 2016;24:S270.

65. Hartz B, Marsh R, Rao K, et al. The minimum required level of donor chimerism in hereditary hemophagocytic lymphohistiocytosis. Blood 2016; 127:3281–3290.

66. Ghosh S, Carmo M, Calero-Garcia M, et al. T-cell gene therapy for perforin deficiency corrects cytotoxicity defects and prevents hemophagocytic lymphohistiocytosis manifestations. J Allergy Clin Immunol 2018;142:904.e3–913.e3.

67. Marcenaro S, Gallo F, Martini S, et al. Analysis of natural killer-cell function in familial hemophagocytic lymphohistiocytosis (FHL): defective CD107a surface expression heralds Munc13-4 defect and discriminates between genetic subtypes of the disease. Blood 2006;108:2316–2323.

68. Krebs P, Crozat K, Popkin D, et al. Disruption of MyD88 signaling suppresses hemophagocytic lymphohistiocytosis in mice. Blood 2011;117:6582–6588.

Received for publication November 19, 2019;
accepted after revision March 19, 2020.

Published online: March 25, 2020.